2018 IEEE International Conference on Robotics and Automation (ICRA)
May 21-25, 2018, Brisbane, Australia

Optimal Path Planning in Time-Varying Flows with Forecasting Uncertainties

Dhanushka Kularatne[1], Hadi Hajieghrary[1] and M. Ani Hsieh[2]

Abstract— **Uncertainties in flow models have to be explicitly considered for effective path planning in marine environments. In this paper, we present two methods to compute minimum expected cost policies and paths over an uncertain flow model. The first method based on a Markov Decision Process computes a minimum expected cost policy while the second graph search based method, computes a minimum expected cost path. A transition probability model is developed to compute the probability of transition from one state to another under a given action. In addition, a method to compute the expected cost of a path when it is executed in an uncertain flow field is also presented. The two methods are used to compute minimum energy paths in an ocean environment and the results are analyzed in simulations.**

I. Introduction

Scientific activities such as migration tracking, characterizing the dynamics of plankton assemblages, measurement of temperature profiles, and monitoring of harmful algae blooms [1] are increasingly being automated using autonomous marine vehicles (AMVs). In order to maximize the utility of these resource constrained vehicles, energy efficient motion strategies need to be developed.

The high inertia environment of the ocean which couples the environmental dynamics to the marine vehicle dynamics, presents a unique opportunity for vehicles to exploit the surrounding flows for more efficient navigation. As such, there is a substantial amount of recent work on determining optimal energy paths in flow fields. Existing work include graph search methods to plan time and energy optimal paths in static [2, 3] and time-varying [4] flow fields. Alternatives to graph search techniques include [5, 6] for computing energy optimal paths in time-varying flows. Lolla *et al.*[7] presented a level set expansion method to find time optimal paths in time-varying flows. This was then extended by Subramani *et al.*[8] to determine the energy optimal paths from the set of time optimal paths obtained from the level set method.

Most of the existing work in the literature on optimal path planning in flow fields, assume that full knowledge of the flow, both in space and time, is available for use in the path planning process. This information could be in the form of flow velocity forecasts or a valid flow velocity model. Such forecasts could be obtained from sources such as the Regional Ocean Model System (ROMS) [9]. However, forecasting ocean phenomena such as current velocities is a complex process and is an active area of research in physical oceanography. Forecasting these phenomena begins with a suite of dynamic models based on theoretical principles, e.g., Navier-Stokes equations. Data from a multitude of sources including satellite observations, high frequency (HF) radar and ship based acoustic measurements, are used to initialize these models and to provide boundary conditions. However, the complexity of the underlying oceanic processes coupled with our limited understanding of their dynamics gives rise to uncertainty in these models. In addition, low spatio-temporal sampling resolutions as well as limited accuracies in the measurement devices themselves, further contribute to errors in the data used to initialize the forecasting models. While data assimilation techniques [10], are widely used to reduce uncertainties from these various sources, existing approaches must assume a model for the underlying process. As such, there is often significant uncertainty associated with the forecast outputs.

In the context of path planning in ocean flows, presence of forecast uncertainties will lead to significant differences between predicted and actual path costs and execution times. Therefore path planning methods should account for these uncertainties and be able to plan for their effects. However, only a handful of authors have studied path planning in ocean flows under forecast uncertainties. Huynh *et al.*[11] proposed a non-linear robust model predictive control (NRMPC) method to compute a minimum energy cost policy under forecast uncertainties in time-varying ocean flows. This method uses a min-max optimization formulation to compute the minimum of the worst case costs. However, the method assumes a bounded uncertainty model and the results are tightly coupled to the kinematic model used for the vehicle. Markov Decision Processes (MDP) have been used by Al-Sabban [12] to compute minimum time paths in a wind-field, by Wolf *et al.*[13] to compute fastest time paths for a balloon in a time-varying wind field, and by Pereira *et al.*[14] to plan paths with minimum risk of collision in an ocean environment. However, none of these works address the problem of minimum energy path planning in time-varying flows.

In this paper, two path planning methods that explicitly consider the flow velocity forecast uncertainties are presented. Both methods consider a minimum energy cost function, and both methods try to minimize the expected cost of a path. The first method uses an MDP formulation to obtain an optimal cost policy and the second method uses a

[1]Dhanushka Kularatne and Hadi Hajieghrary are with the Scalable Autonomous Systems Lab, Drexel University, Philadelphia, PA 19104, USA.{dnk32, hh449}@drexel.edu. [2]M. Ani Hsieh is with the GRASP Laboratory, University of Pennsylvania, Philadelphia, PA 19104, USA. m.hsieh@seas.upenn.edu. This work was supported by the National Science Foundation (NSF) grants IIS-1253917 and CMMI-1462825.

graph based approach to compute a minimum expected cost path. The distinction between a policy and a path becomes important during actual execution of the policy/path. With an optimal policy, the AMV will compute and apply an optimal control based on its current state. In contrast, with an optimal path (parameterized by time), a tracking controller will be executed on the AMV to follow the path. The main contributions of this paper are 1) two methods that could be used to compute optimal paths/policies using uncertain flow velocity forecasts, 2) a probabilistic transition model for an autonomous surface vehicle (ASV) in an uncertain flow field, and 3) a method to compute expected cost and variance of a given path in an uncertain flow field. In contrast to existing work [12, 13, 14], our methods consider a more general cost function, time-varying flows and a more general uncertainty model.

The rest of the paper are organized as follows. Section II presents the problem preliminaries, section III presents the MDP based minimum energy planner and section IV presents the graph based minimum expected cost path planner. Simulation results are presented in Section V. The paper concludes with a discussion and directions for future work in Section VI.

II. Preliminaries

A. Environment and Flow Model

We consider a 2-D aquatic environment $\mathbb{W} \subseteq \mathbb{R}^2$, subject to a time-varying flow field $\tilde{\mathbf{V}}_\mathbf{f} : \mathbb{W}_T \mapsto \mathbb{R}^2$, where $\mathbb{W}_T = \mathbb{W} \times [\underline{t},\ \bar{t}]$ and $[\underline{t},\ \bar{t}] \subset \mathbb{R}_{\geq 0}$ denotes the time interval under consideration. As such, for $\mathbf{x} \in \mathbb{W}$ and $t \in [\underline{t},\ \bar{t}]$, $\tilde{\mathbf{V}}_\mathbf{f}(\mathbf{x},t) = \left[\tilde{V}_{fx}(\mathbf{x},t),\ \tilde{V}_{fy}(\mathbf{x},t)\right]^T$ denotes the flow velocity, with $\tilde{V}_{fx}$ and $\tilde{V}_{fy}$ denoting the components of the flow vector in the inertial frame. The speed of the flow is given by $\tilde{V}_f(\mathbf{x},t) = \|\tilde{\mathbf{V}}_\mathbf{f}(\mathbf{x},t)\|$ and the maximum flow speed encountered in the domain is given by $V_{fm} = \max_{\mathbf{x}\in\mathbb{W},\ t\in[\underline{t},\ \bar{t}]} \tilde{V}_f(\mathbf{x},t)$.

Ocean flow velocity forecasts obtained for example from the ROMS database, contain separate predictions for the zonal current (x-direction) and the meridional current (y-direction). As such, it is assumed that forecast uncertainties affect the x-y current components independently and that the uncertainty in the flow velocity vector can be represented by the following model.

$$\tilde{V}_{fx}(\mathbf{x},t) = V_{fx}(\mathbf{x},t) + \eta_{fx}(t) \tag{1a}$$

$$\tilde{V}_{fy}(\mathbf{x},t) = V_{fy}(\mathbf{x},t) + \eta_{fy}(t), \tag{1b}$$

where V_{fx} and V_{fy} represent the deterministic flow velocity components, and η_{fx} and η_{fy} represent forecast uncertainties in the x and y directions respectively. It is assumed that these noise components are drawn from independent Gaussian distributions $\eta_{fx} \sim \mathcal{N}(0, \sigma_{fx}^2)$ and $\eta_{fy} \sim \mathcal{N}(0, \sigma_{fy}^2)$. This is a common model used in the literature to represent uncertainty in flow velocity forecasts [14, 11]. In practice, historical nowcasts and forecasts could be used to compute σ_{fx} and σ_{fy}. It is further assumed that the deterministic x-y components of the flow velocities, *i.e.,* V_{fx} and V_{fy}, are independent of each other.

B. Vehicle Model

We assume a holonomic kinematic model for the autonomous marine vehicle (AMV). This is a reasonable assumption when the dimensions of the AMV are small when compared with the dimensions of the flow structures. Using this model, the net velocity of the vehicle with respect to the inertial frame is given by

$$\mathbf{V_{net}}(\mathbf{x},t) = \tilde{\mathbf{V}}_\mathbf{f}(\mathbf{x},t) + \mathbf{V_{still}}(\mathbf{x},t), \tag{2}$$

where $\mathbf{V_{still}} = [V_{still,x},\ V_{still,y}]^T$ is the velocity of the vehicle with respect to the flow, *i.e.,* $\mathbf{V_{still}}$ is the "thrust" vector of the vehicle. The velocity magnitudes are respectively represented as, $V_{net} = \|\mathbf{V_{net}}\|$, $V_f = \|\tilde{\mathbf{V}}_\mathbf{f}\|$, $V_{still} = \|\mathbf{V_{still}}\|$. We further assume that that the actuation capability of the vehicle is limited and that its maximum speed is lower than the speed of the surrounding flow *i.e.,* $V_{still}(\mathbf{x},t) \leq V_{max} < V_{fm}$.

C. Cost Function

The objective of this work is to develop methods that could be used to compute minimum energy paths in time-varying flow fields with an uncertain flow velocity description. Thus we consider a cost function that represents the energy consumption of the AMV. The total energy consumed by the AMV is considered to be $E_{total} = E_{hotel} + E_{drag}$, where E_{hotel} is the energy required to operate the vehicle's computing and sensor systems independent of propulsion, and E_{drag} is the energy expended to overcome drag forces exerted by the fluid. Assuming a constant power usage K_h by the computing and sensor systems gives $E_{hotel} = \int_{t_s}^{t_g} K_h dt$. The drag force F_d encountered by the AMV along a path $\Gamma(t)$ is given by $F_d(t) = K_d V_{still}^{\alpha-1}(\Gamma(t),t)$ where K_d is the drag coefficient and $\alpha \in \{2,3,...\}$. If $\alpha = 2$ the drag is linear, if $\alpha = 3$ the drag is quadratic, and so on. This leads to $E_{drag} = \int_{t_s}^{t_g} K_d V_{still}^{\alpha}(\Gamma(t),t) dt$. Thus, the cost of a path is given by

$$C(\Gamma) = \int_{t_s}^{t_g} K_h + K_d V_{still}^{\alpha}(\Gamma(t),t) dt, \tag{3}$$

and the cost of a small path segment $[dx, dy]^T$, traversed in time dt is given by,

$$dc = \left(K_h + K_d V_{still}^{\alpha}(\Gamma(t),t)\right) dt. \tag{4}$$

where V_{still} is computed using (2) with $\mathbf{V_{net}} = [\frac{dx}{dt},\ \frac{dy}{dt}]^T$. Note that, K_h and K_d can also be thought of as weighting parameters between minimum time paths and minimum energy paths. If a minimum time path is required, we could set $K_d = 0$ and proceed, and vice versa. If exact energy minimization is required, actual values for K_h and K_d should be used.

D. Probability Distributions

The position of a particle initially at $\mathbf{x_i} = [x_i, y_i]^T$ at time t_i, after it is advected by the uncertain flow given in (1) for a time interval dT, is given by,

$$\tilde{x_i} = x_i + \tilde{V}_{fx}(\mathbf{x_i}, t_i) dT \tag{5a}$$

$$\tilde{y_i} = y_i + \tilde{V}_{fy}(\mathbf{x_i}, t_i) dT. \tag{5b}$$

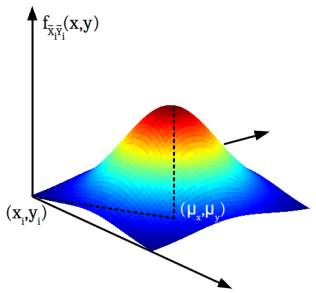

Fig. 1: Probability density function of the position of a particle advected by the uncertain flow. The PDF has a bivariate Gaussian distribution with mean $[\mu_{\tilde{x}},\mu_{\tilde{y}}]^T$.

From (1) and (5), it can be easily seen that $\tilde{x}_i$ and $\tilde{y}_i$ have normally distributed probability density functions (PDFs) $f_{\tilde{X}_i}(\tilde{x}_i)$ and $f_{\tilde{Y}_i}(\tilde{y}_i)$ respectively, *i.e.,* $\tilde{X}_i \sim \mathcal{N}(\mu_{\tilde{x}_i},\sigma_{\tilde{x}}^2)$ and $\tilde{Y}_i \sim \mathcal{N}(\mu_{\tilde{y}_i},\sigma_{\tilde{y}}^2)$ where

$$\mu_{\tilde{x}_i} = x_i + V_{fx}(\mathbf{x_i},t_i)dT_i, \quad \sigma_{\tilde{x}} = \sigma_{fx}dT \tag{6a}$$

$$\mu_{\tilde{y}_i} = y_i + V_{fy}(\mathbf{y_i},t_i)dT_i, \quad \sigma_{\tilde{y}} = \sigma_{fy}dT. \tag{6b}$$

The vector$[\mu_{\tilde{x}_i},\mu_{\tilde{y}_i}]^T$ can also be interpreted as the position of the particle when it is advected by the fully deterministic flow. Note that the standard deviations are independent of the initial position $\mathbf{x}_i$, and hence the i subscripts are dropped. Since it is assumed that V_{fx} and V_{fy} as well as η_{fx} and η_{fy} are independent, $\tilde{x}_i$ and $\tilde{y}_i$ are also independent. Thus the joint probability density function of $\tilde{x}_i$ and $\tilde{y}_i$ is given by

$$f_{\tilde{X}_i\tilde{Y}_i}(\tilde{x}_i,\tilde{y}_i) = f_{\tilde{X}_i}(\tilde{x}_i)f_{\tilde{Y}_i}(\tilde{y}_i). \tag{7}$$

This implies that the region of space reachable by a particle advected by the uncertain flow over a time step dT has a bivariate Gaussian distribution with mean $[\mu_{\tilde{x}_i},\mu_{\tilde{y}_i}]^T$ and covariance matrix $\begin{bmatrix} \sigma_{\tilde{x}}^2 & 0 \\ 0 & \sigma_{\tilde{y}}^2 \end{bmatrix}$ (see Fig. 1).

Similarly, the position of an AMV initialized at $\mathbf{x}_i = [x_i,y_i]^T$ at time time t_i, under the action of a thrust vector $\mathbf{V_{still_j}} = [V_{still_j,x}, V_{still_j,y}]^T$ for time dT, is given by,

$$x_j = x_i + (\tilde{V}_{fx}(\mathbf{x_i},t_i) + V_{still_j,x})dT = \tilde{x}_i + V_{still_j,x}dT \tag{8a}$$

$$y_j = y_i + (\tilde{V}_{fy}(\mathbf{x_i},t_i) + V_{still_j,y})dT = \tilde{y}_i + V_{still_j,y}dT. \tag{8b}$$

Thus, it can be seen that under the considered uncertainty model, the AMV coordinates x_j, y_j have normally distributed PDFs $f_{X_j}(x_j)$ and $f_{Y_j}(y_j)$ respectively, *i.e.,* $X_j \sim \mathcal{N}(\mu_{\tilde{x}_i} + V_{still_j,x}dT,\ \sigma_{\tilde{x}}^2)$ and $Y_j \sim \mathcal{N}(\mu_{\tilde{y}_i} + V_{still_j,y}dT,\ \sigma_{\tilde{y}}^2)$. Note that since $V_{still_j,x}$ and $V_{still_j,y}$ are independent, x_j and y_j are independent as well. Thus, similar to a particle advected by just the flow, the position of the AMV under this model also has a bivariate Gaussian distribution given by,

$$f_{X_jY_j}(x,y) = f_{X_j}(x)f_{Y_j}(y). \tag{9}$$

III. MDP PLANNER

Due to the uncertainty in the flow velocity forecasts, the position of the AMV after applying a given control vector $\mathbf{V_{still}}$ for a time interval of dT, cannot be determined deterministically. The position of the AMV is now a random variable whose properties are determined by the uncertainty in the flow. Thus, in contrast to the deterministic case, the next control action that will minimize the overall path cost cannot be computed *a priori*. In such scenarios what is required is an optimal control policy that minimizes the expected cost, instead of a set of controls that is determined *a priori*. Such a minimum expected cost policy could be determined using a MDP planner. For a given state, the MDP determines what the control needs to be in order to minimize the expected cost to goal. An MDP is a tuple (S,A,P,R), where S is the set of states, A is the set of allowed actions at each state, P represents the set of transition probabilities, and $R : S \times A \mapsto \mathbb{R}$ is a reward function that maps action a at state s to a reward $R(s,a)$. The transition probability $P(s'|s,a)$ denotes the probability of ending at state s' after taking action a at state s.

A. MDP formulation

States (S): The spatio-temporal workspace $\mathbb{W}_T$ is uniformly discretized into a grid (see Fig. 2a), where each node represents a state s of the system and is identified by the pair $(\mathbf{x},t)$. The set S consists of all the nodes in the gridded representation of $\mathbb{W}_T$.

Actions (A): The action set A at each state consists of the allowable controls at that state. It is assumed that all states have the same set of allowable actions and is given by $\{\mathbf{V_{still_1}},\mathbf{V_{still_2}},\cdots\mathbf{V_{still_m}}\}$. Furthermore, each action would be applied for a single dT time interval. Therefore, when an action a is applied at state s, only states that are one time step away from s can be reached, *i.e.,* all states reached from $s = (\mathbf{x},t)$ will have a time coordinate $t + dT$ (see Fig. 2a).

Transition probabilities (P): Consider a state s_i with coordinates $(\mathbf{x_i},t_i)$, at which an action a_j is applied. Since, every action is applied for exactly one time step, $P(s'|s_i,a_j) = 0$ for states $s' = (\mathbf{x}',t')$ with time coordinate $t' \neq t_i + dT$. For states with $t' = t_i + dT$, consider a state $s' = (\mathbf{x}',t_i + dT)$ reached by applying an action $a_j = \mathbf{V_{still_j}}$ at state $s_i = (\mathbf{x_i},t_i)$. Since the 2-D space is uniformly discretized with resolutions dx and dy in the x and y directions respectively, the probability of reaching s' is given by the total probability of reaching a square region with dimensions $dx \times dy$ centered around $\mathbf{x}'$ (see Fig. 2b). Therefore, the probability of reaching s' from s_i under an action a_j is given by,

$$P(s'|s_i,a_j) = \int_{y'-dy/2}^{y'+dy/2}\int_{x'-dx/2}^{x'+dx/2} f_{X_jY_j}(x,y)dxdy. \tag{10}$$

This probability is equivalent to reaching a square area around the intermediate point $\tilde{\mathbf{x}}_\mathbf{i}$ which is reached by the action of the flow alone (area shaded in blue in Fig. 2b). For a state $s' = (\mathbf{x}',t')$ reached under an action $a_j = \mathbf{V_{still_j}}$, this intermediate point is given by,

$$\tilde{\mathbf{x}}_\mathbf{i} = \mathbf{x}' - \mathbf{V_{still_j}}dT, \tag{11}$$

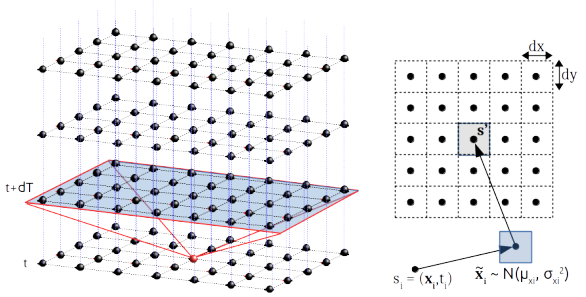

(a) (b)

Fig. 2: (a) The workspace $\mathbb{W}_T$ is discretized uniformly. Each node in the grid represents a state. Under a given action $a \in A$ at state s (red), only the states in the immediate time step (shaded slice) are accessible. (b) The probability of reaching state s' from s_i under an action a_j is considered to be equal to the probability of reaching the grey shaded area around $\mathbf{x}'$. It is also equivalent to the probability of reaching area shaded in blue under the action of the flow alone.

and the corresponding transition probability is given by,

$$P(s'|s_i,a_j) = \int_{\tilde{y}_i-dy/2}^{\tilde{y}_i+dy/2}\int_{\tilde{x}_i-dx/2}^{\tilde{x}_i+dx/2} f_{\tilde{X}_i\tilde{Y}_i}(x,y)dxdy$$
$$= \frac{1}{2\pi\sigma_{\tilde{x}}\sigma_{\tilde{y}}}\int_{\tilde{y}_i-dy/2}^{\tilde{y}_i+dy/2}\int_{\tilde{x}_i-dx/2}^{\tilde{x}_i+dx/2} e^{-\left[\frac{(x-\mu_{\tilde{x}_i})^2}{2\sigma_{\tilde{x}}^2}+\frac{(y-\mu_{\tilde{y}_i})^2}{2\sigma_{\tilde{y}}^2}\right]}dxdy. \quad (12)$$

It can be shown that, for a fixed $\sigma_{\tilde{x}}$ and $\sigma_{\tilde{y}}$, the integral given in (12) only depends on the differences $(\tilde{x}_i-\mu_{\tilde{x}_i})$ and $(\tilde{y}_i-\mu_{\tilde{y}_i})$. Thus, in the implementation, the above integral is precomputed on a uniformly discretized $(\tilde{x}_i-\mu_{\tilde{x}_i})\times(\tilde{y}_i-\mu_{\tilde{y}_i})$ grid, and linear interpolation is used on the gridded values to approximate the value of the integral.

Reward function (R): The energy cost function given in (4) is used as the reward function. With this reward function, the MDP planner will compute a policy with minimum expected energy cost to reach the target from each state.

B. Computation of the optimal policy

Consider a control policy π composed of an infinite sequence of decision functions $\{\pi_0,\pi_1,\cdots\}$, where each $\pi_i : S \mapsto A$ is function that maps a state to an admissible action. However, since the transitions between states are probabilistic, it is not possible to directly compute the cost associated with this control policy. Thus, the cost associated with a given policy π that starts from a state s, is defined as the expected cumulative cost incurred by π, and is given by $J_\pi(s_i) = E\left[\sum_{k=o}^{\infty} R\big(s_k,\pi_k(s_k)\big)\middle| s_0 = s_i\right]$ where the E denotes the expectation with respect to the transition probabilities P. The optimal cost policy π^* satisfies, $J^*(s_i) = J_{\pi^*}(s_i) \le J_\pi(s_i)$ for $\forall s_i \in S$. For a given target state s_t it has been shown that [15] the optimal cost vector satisfies

$$J^*(s_i) = \begin{cases} 0 & s_i = s_t, \\ \min\limits_{a_j\in A} \quad R(s_i,a_j) + \sum\limits_{s'\in S} P(s'|s_i,a_j)J^*(s') & s_i \neq s_t \end{cases} \quad (13)$$

and that the optimal policy is given by,

$$\pi^*(s_i) = \underset{a_j\in A}{argmin} \quad R(s_i,a_j) + \sum_{s'\in S} P(s'|s_i,a_j)J^*(s'). \quad (14)$$

The most common method of solving (13) is value iteration, where the value of the cost vector J^* is updated iteratively. At each iteration, the value of the cost vector is updated as,

$$J_{k+1}(s_i) = \begin{cases} 0 & s_i = s_t \\ \min\limits_{a_j\in A} \quad R(s_i,a_j) + \sum\limits_{s'\in S} P(s'|s_i,a_j)J_k(s') & s_i \neq s_t \end{cases} \quad (15)$$

$\forall s_i \in S$ with $J_0(s_i) = \infty$ for $s_i \neq s_t$. It is guaranteed that the value iteration converges, *i.e.*, $J_k(s_i) \to J^*(s_i)$ for all $s_i \in S$ [15]. In practice, the value iteration is terminated when $\|J_{k+1}(s_i) - J_k(s_i)\| < \epsilon$. The final J_k is used in (14) to compute the optimal control policy.

Note that the summation in (15) is over all states in S. However, since $P(s'|s_i,a_j) = 0$ when $t' \neq t_i + dT$, the summation needs to be done only over a subset of S. The cardinality of this subset can be further reduced by considering the properties of the transition probability function given in (12). It can be seen that $P(s'|s_i,a_j) \ll 1$ when $\frac{\|\tilde{x}_i-\mu_{\tilde{x}_i}\|}{\sigma_{\tilde{x}}} \gg 1$ or when $\frac{\|\tilde{y}_i-\mu_{\tilde{y}_i}\|}{\sigma_{\tilde{y}}} \gg 1$. Therefore the subset $\tilde{S}_{ij} \subset S$ over which the summation is carried out is considered to be

$$\tilde{S}_{ij} = \{s=(\mathbf{x},t)\big| t = t_i + dT,\ \|x - V_{still_j,x}dT - \mu_{\tilde{x}_i}\| \le N_\sigma\sigma_{\tilde{x}},$$
$$\|y - V_{still_j,y}dT - \mu_{\tilde{y}_i}\| \le N_\sigma\sigma_{\tilde{y}}\} \quad (16)$$

where $N_\sigma > 1$ determines the number of standard deviations considered for the computations. Generally, $N_\sigma = 2$ captures a significant portion of the probability distribution. This reduction will greatly reduce the computation time of the cost vector J_k.

IV. Minimum Expected Cost Planner

In this section a graph based minimum expected cost planner is developed. First the expected cost of a path when it is executed in an uncertain flow field is computed.

A. Expected path cost

Consider a path segment from $(\mathbf{x_i},t_i)$ to $(\mathbf{x_j},t_j)$ of path $\{(\mathbf{x_0},t_0),(\mathbf{x_1},t_1),\cdots,(\mathbf{x_N},t_N)\}$ in $\mathbb{W}_T$, where $t_{i+1} = t_i + dT$. Thus, note that $t_j = t_i + dT$. If a fully deterministic flow is considered, the components of $\mathbf{x}_j$ are given by,

$$x_j = x_i + V_{fx}(\mathbf{x_i},t_i)dT_i + V_{still,x}(\mathbf{x_i},t_i)dT = \mu_{\tilde{x}_i} + V_{still_i,x}dT \quad (17a)$$

$$y_j = y_i + V_{fy}(\mathbf{x_i},t_i)dT_i + V_{still,y}(\mathbf{x_i},t_i)dT = \mu_{\tilde{y}_i} + V_{still_i,y}dT. \quad (17b)$$

where $\mu_{\tilde{x}_i}$ and $\mu_{\tilde{y}_i}$ are given in (6), and $V_{still_i,x}$ and $V_{still_i,y}$ are the components of the thrust vector $\mathbf{V_{still_i}}$ required to reach $\mathbf{x}_j$ from $\mathbf{x}_i$ when the flow is fully known. However, when the flow is uncertain, the actual magnitude of the thrust vector required to reach $\mathbf{x}_j$ will depend on the intermediate flow driven location $\tilde{\mathbf{x}} = [\tilde{x},\tilde{y}]^T$ of the AMV (see Fig. 3). Using (8) and (17), the components of this actual thrust vector can be written as,

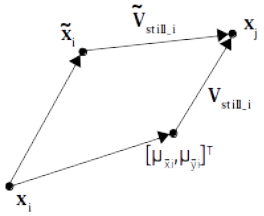

Fig. 3: In a fully known flow, the intermediate point is $[\mu_{\tilde{x}_i}, \mu_{\tilde{y}_i}]^T$ and $\mathbf{x_j}$ could be reached by applying a thrust vector $\mathbf{V_{still_i}}$. When the flow is uncertain, the intermediate point $\tilde{\mathbf{x}}_\mathbf{i}$ is a random variable and hence the actual thrust vector $\tilde{\mathbf{V}}_{\mathbf{still_i}}$ required to drive the AMV to $\mathbf{x_j}$ is also a random variable.

$$\tilde{V}_{still_i,x} = \frac{x_j - \tilde{x}}{dT} = \frac{\mu_{\tilde{x}_i} + V_{still_i,x} dT_i - \tilde{x}}{dT} \tag{18a}$$

$$\tilde{V}_{still_i,y} = \frac{y_j - \tilde{y}}{dT} = \frac{\mu_{\tilde{y}_i} + V_{still_i,y} dT_i - \tilde{y}}{dT}. \tag{18b}$$

Since $\tilde{x}$ and $\tilde{y}$ are random variables, $\tilde{V}_{still_i,x}$ and $\tilde{V}_{still_i,y}$ are also random variables, with expected values,

$$E[\tilde{V}_{still_i,x}] = V_{still_i,x} + \frac{\mu_{\tilde{x}_i} - E[\tilde{x}]}{dT} = V_{still_i,x} \tag{19a}$$

$$E[\tilde{V}_{still_i,y}] = V_{still_i,y} + \frac{\mu_{\tilde{y}_i} - E[\tilde{y}]}{dT} = V_{still_i,y} \tag{19b}$$

and with variances

$$V[\tilde{V}_{still_i,x}] = \frac{V[\tilde{x}]}{dT^2} = \frac{\sigma^2_{\tilde{x}}}{dT^2} = \sigma^2_{fx} \tag{20a}$$

$$V[\tilde{V}_{still_i,y}] = \frac{V[\tilde{y}]}{dT^2} = \frac{\sigma^2_{\tilde{y}}}{dT^2} = \sigma^2_{fy}. \tag{20b}$$

Therefore, $\tilde{V}_{still_i,x}$ and $\tilde{V}_{still_i,y}$ have normally distributed PDFs $f_{\tilde{V}_{still_i,x}}(\tilde{V}_{still_i,x})$ and $f_{\tilde{V}_{still_i,y}}(\tilde{V}_{still_i,y})$ respectively, *i.e.,* $\tilde{V}_{still_i,x} \sim \mathcal{N}(V_{still_i,x}, \sigma^2_{fx})$ and $\tilde{V}_{still_i,y} \sim \mathcal{N}(V_{still_i,y}, \sigma^2_{fy})$. Furthermore, since it is assumed that all processes in the x and y directions are independent, $\tilde{V}_{still_i,x}$ and $\tilde{V}_{still_i,y}$ are also independent. Thus, the joint probability distribution can be written as

$$f_{\tilde{V}_{still_i,x}\tilde{V}_{still_i,y}}(\tilde{V}_{still_i,x}, \tilde{V}_{still_i,y}) = f_{\tilde{V}_{still_i,x}}(\tilde{V}_{still_i,x}) f_{\tilde{V}_{still_i,y}}(\tilde{V}_{still_i,y}).$$

The cost incurred to traverse this path segment under an uncertain flow description is given by

$$dC_i = \left(K_h + K_d \tilde{V}^\alpha_{still_i}\right) dT.$$

Using the joint PDF of $\tilde{V}_{still_i,x}$ and $\tilde{V}_{still_i,y}$, the expected value of $\tilde{V}^\alpha_{still_i}$ is given by

$$E[\tilde{V}^\alpha_{still_i}] = \int\int \left(\tilde{V}^2_{still_i,x} + \tilde{V}^2_{still_i,y}\right)^{\alpha/2} f_{\tilde{V}_{still_i,x}}(\tilde{V}_{still_i,x}) \, f_{\tilde{V}_{still_i,y}}(\tilde{V}_{still_i,y}) d\tilde{V}_{still_i,x} d\tilde{V}_{still_i,y}, \tag{21}$$

which can be expanded using the definitions of $f_{\tilde{V}_{still_i,x}}(\tilde{V}_{still_i,x})$ and $f_{\tilde{V}_{still_i,y}}(\tilde{V}_{still_i,y})$ to give

$$E[\tilde{V}^\alpha_{still_i}] = \int\int \frac{\left(\hat{x}^2 + \hat{y}^2\right)^{\alpha/2}}{2\pi\sigma_{fx}\sigma_{fy}} e^{-\left[\frac{(\hat{x} - V_{still_i,x})^2}{2\sigma^2_{fx}} + \frac{(\hat{y} - V_{still_i,y})^2}{2\sigma^2_{fy}}\right]} d\hat{x} d\hat{y}, \tag{22}$$

where $\hat{x}$ and $\hat{y}$ have been used in place of $\tilde{V}_{still_i,x}$ and $\tilde{V}_{still_i,y}$ for clarity of exposition. Similarly, the expected value of $\tilde{V}^{2\alpha}_{still_i}$ can be expressed as,

$$E[\tilde{V}^{2\alpha}_{still_i}] = \int\int \frac{\left(\hat{x}^2 + \hat{y}^2\right)^{\alpha}}{2\pi\sigma_{fx}\sigma_{fy}} e^{-\left[\frac{(\hat{x} - V_{still_i,x})^2}{2\sigma^2_{fx}} + \frac{(\hat{y} - V_{still_i,y})^2}{2\sigma^2_{fy}}\right]} d\hat{x} d\hat{y}, \tag{23}$$

which can be used to find the variance of $\tilde{V}^\alpha_{still_i}$,

$$V[\tilde{V}^\alpha_{still_i}] = E[\tilde{V}^{2\alpha}_{still_i}] - E[\tilde{V}^\alpha_{still_i}]^2. \tag{24}$$

Thus the expected cost and the cost variance of this path segment are,

$$E[dC_i] = \left(K_h + K_d E[\tilde{V}^\alpha_{still_i}]\right) dT \tag{25a}$$

$$V[dC_i] = K_d^2 dT^2 V[\tilde{V}^\alpha_{still_i}]. \tag{25b}$$

where $E[\tilde{V}^\alpha_{still_i}]$ and $V[\tilde{V}^\alpha_{still_i}]$ are given by (22) and (24) respectively. And the expected cost of the complete path $\Gamma_G = \{(\mathbf{x_0}, t_0), (\mathbf{x_1}, t_1), \cdots, (\mathbf{x_N}, t_N)\}$ is

$$E[C(\Gamma_G)] = \sum_{i=0}^{N-1} E[dC_i] \tag{26}$$

and assuming that the cost of each path segment is independent from each other (Markovian assumption), the variance of the path cost is

$$V[C(\Gamma_G)] = \sum_{i=0}^{N-1} V[dC_i]. \tag{27}$$

For the special case when $\alpha = 2$ (linear drag), the expressions for the expected cost and cost variance of a path segment can be further simplified. When $\alpha = 2$, $\tilde{V}^\alpha_{still_i} = \tilde{V}^2_{still_i} = \tilde{V}^2_{still_i,x} + \tilde{V}^2_{still_i,y}$. Thus using the independence of $\tilde{V}_{still_i,x}$ and $\tilde{V}_{still_i,y}$, $E[\tilde{V}^\alpha_{still_i}]$ can be written as

$$E[\tilde{V}^2_{still_i}] = E[\tilde{V}^2_{still_i,x}] + E[\tilde{V}^2_{still_i,y}].$$

Similarly, after some simple calculations $V[\tilde{V}^\alpha_{still_i}]$ can be written as

$$V[\tilde{V}^2_{still_i}] = E[\tilde{V}^4_{still_i,x}] + E[\tilde{V}^4_{still_i,y}] - E[\tilde{V}^2_{still_i,x}]^2 - E[\tilde{V}^2_{still_i,y}]^2.$$

It can be easily shown that for a normally distributed random variable $X \sim \mathcal{N}(\mu, \sigma^2)$,

$$E[X^2] = \mu^2 + \sigma^2 \tag{28a}$$

$$E[X^4] = 3\sigma^4 + 6\mu^2\sigma^2 + \mu^4. \tag{28b}$$

Thus,

$$E[\tilde{V}^2_{still_i}] = V^2_{still_i,x} + \sigma^2_{fx} + V^2_{still_i,y} + \sigma^2_{fy} = V^2_{still_i} + \sigma^2_{fx} + \sigma^2_{fy}$$

and after some tedious simplifications

$$V[\tilde{V}^2_{still_i}] = 2(\sigma^4_{fx} + \sigma^4_{fy}) + 4(V^2_{still_i,x}\sigma^2_{fx} + V^2_{still_i,y}\sigma^2_{fy}).$$

Thus, when $\alpha = 2$, (25b) simplifies to

$$V[dC_i] = 2K_d^2 dT^2 \left(\sigma^4_{fx} + \sigma^4_{fy} + 2(V^2_{still_i,x}\sigma^2_{fx} + V^2_{still_i,y}\sigma^2_{fy})\right),$$

and (25a) simplifies to

$$\begin{aligned} E[dC_i] = & \quad \big(K_h + K_d(V_{still_i}^2 + \sigma_{fx}^2 + \sigma_{fy}^2)\big)dT \\ = & \quad \big(K_h + K_d(\sigma_{fx}^2 + \sigma_{fy}^2) + K_d V_{still_i}^2\big)dT \\ = & \quad \big(\tilde{K}_h + K_d V_{still_i}^2\big)dT \end{aligned} \tag{29}$$

where $\tilde{K}_h = K_h + K_d(\sigma_{fx}^2 + \sigma_{fy}^2)$. Thus the uncertainty in the flow, increases the constant power requirement of the AMV by $K_d(\sigma_{fx}^2 + \sigma_{fy}^2)$. Furthermore, the total expected path cost becomes $E[C(\Gamma_G)] = C(\Gamma_G) + K_d(\sigma_{fx}^2 + \sigma_{fy}^2)(t_N - t_0)$. Thus, under the effect of uncertainty, the total path cost has increased by $K_d(\sigma_{fx}^2 + \sigma_{fy}^2)(t_N - t_0)$, which can be thought of as the total energy required to overcome the drag forces enacted by the uncertainty in the flow field.

B. Graph based minimum expected cost planner

Equations (25a) and (22) show that $E[dC_i]$ can be computed, if σ_{fx}, σ_{fy} and the thrust vector $\mathbf{V_{still}}_i$ required to traverse the path segment in a deterministic flow, are known. Thus, $E[dC_i]$ can be used as the cost function in a graph based method to compute the minimum expected cost path.

The graph search method used in this work is called the single time step search (STS) method. During graph construction, the STS method considers the reachable space from a given node $s_i = (\mathbf{x}_i, t_i)$ in a single time step dT, under the influence of both the vehicle actuation and the flow velocity at s_i. In 2D space, this reachable space is demarcated by a circle of radius $V_{max}dT$ centered at $\tilde{\mathbf{x}} = \mathbf{x}_i + \mathbf{V_f}(\mathbf{x}_i, t_i)dT$. In the STS graph, this reachable space is represented by a hexagonal lattice of vertices, centered at $\tilde{\mathbf{x}}$ with $2n+1$ vertices along the main axis (see 4a). The $m = 3n^2 + 3n + 1$ number of vertices in this lattice are added to the neighbor set $\mathcal{N}(s_i)$ of s_i. For each $s_j \in \mathcal{N}(s_i)$, an edge $e_{ij} = (s_i, s_j)$ and a vertex s_j is added to the graph if the vertex is not obstructed by an obstacle. All the vertices in $\mathcal{N}(s_i)$ will have the same time coordinate $s_j = s_i + dT$. The inter-vertex spacing of the neighbor lattice is $dx = V_{max}dT/n$. The graph is constructed by repeating this process at each node expansion (see Fig. 4b), and the node expansion is guided by the Dijkstra algorithm. In order to use a heuristic search method like A*, a suitable heuristic for the expected cost to reach the goal has to be found. The search is stopped when the target node s_t is reached. Additional information about the STS method can be found in [16].

Note that since the same set of m thrust vectors are used at each node expansion, $E[dC]$ can be precomputed using (22) for each of those thrust vectors. In the case when $\alpha = 2$, $E[dC]$ canbe directly computed by replacing K_h with $\tilde{K}_h = K_h + K_d(\sigma_{fx}^2 + \sigma_{fy}^2)$ in the cost function.

V. Simulation Results

The planners were used to compute optimal policies/paths in the Santa Barbara Bay off the coast of California, using flow velocity forecasts obtained from the Regional Ocean Model System (ROMS). The Southern California Coastal Ocean Observing System (SCCOOS) generates these hourly ocean current forecasts everyday and each forecast is for 72 hours [9]. The data generated on July 7 and July 8 2016 were used. The ROMS data has a $3km \times 3km \times 1hr$ spatio-temporal resolution and linear interpolation was used to obtain flow velocities at intermediate coordinates. The maximum and mean flow speeds encountered in the domain were respectively $0.73m/s$ and $0.18m/s$. The standard deviations of the flow velocity forecasts were set at half the mean flow speed, *i.e.*, $\sigma_{fx} = \sigma_{fy} = V_{mean}/2 = 0.09m/s$. All simulations were for a path between $[20,\ 50]^T km$ and $[50,\ 40]^T km$, and were run on a Linux Core I-7 3.4GHz PC with 16GB of RAM, with cost function parameters set at $K_h = 0.0005$, $K_d = 1$ and $\alpha = 2$.

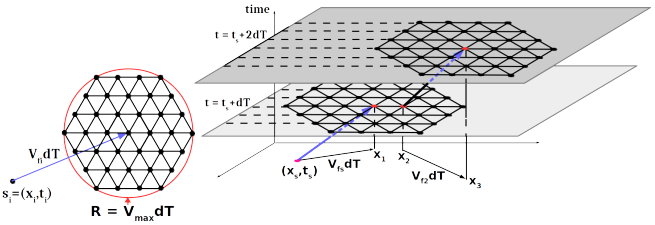

(a) (b)

Fig. 4: (a) The reachable space from s_i is a circle of radius $V_{max}dT$ centered at $\tilde{\mathbf{x}}$. A hexagonal lattice of vertices is used to represent this space in the graph. In this case $n = 3$. (b) Construction of the graph using the STS method. All the vertices reachable within a single time step from the base node are considered as neighbors.

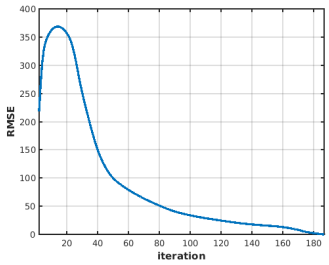

Fig. 5: Root Mean Square Error (RMSE) between successive iterations of the cost vector J_k. The value iteration converged in 185 iterations.

A. MDP planner

The optimal cost vector J^* was computed using a workspace discretized with $dx = dy = 200m$ and $dT = 1000s$. This created a grid containing $191 \times 111 \times 186 = 3,943,386$ states for the considered space-time bounds. The transition probabilities given in (12) were computed on a $(\tilde{x}_i - \mu_{\tilde{x}_i}) \times (\tilde{y}_i - \mu_{\tilde{y}_i})$ grid uniformly discretized at $18m$ intervals and $N_\sigma = 5$ was selected. Value-iteration given in (15) was used to compute the cost vector J^* and it converged in 185 iterations (see Fig. 5). Due to the large number of states, each iteration took on average $257s$ (at each iteration $J_k(s)$ has to be computed for all states), which resulted in a convergence time of approximately 13 hours.

The converged cost vector was used in (14) to obtain the optimal cost policy. A path realized using this policy will depend on the actual flow velocities encountered at each state. Thus, the obtained paths will have a probabilistic distribution

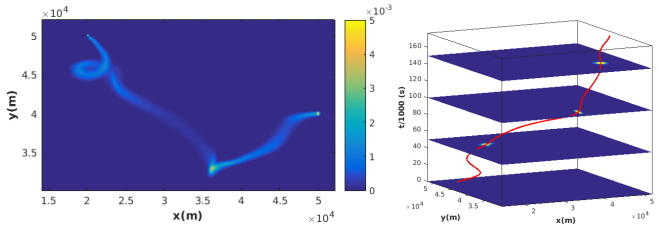

(a) (b)

Fig. 6: (a) 2D histogram of 100,000 paths computed using the MDP planner. (b) Histogram of the paths at different time instances and the average path of the 100,000 realizations (red). The average path was obtained using the weighted mean of the histogram at each time step.

in space and as such, histograms of path realizations were used to obtain a mean path. Fig. 6a shows the 2D histogram of 100,000 path realizations obtained using the MDP planner. Fig. 6b shows histograms at different time instances and the average path for these 100,000 realizations. The average path was obtained by considering the weighted average of the histogram at each time step.

Remark 1: The MDP planner computes an optimal policy. The control action to take at a given state will be computed '*in-situ*' using this optimal cost policy, and the computed control action will be executed by the vehicle. However, unless the model used for the AMV is very accurate, this control cannot be directly executed by the vehicle. Instead, the vehicle will use its lower level controllers to 'follow' this higher level control. Thus, in addition to flow uncertainties, uncertainties and errors in the control stack will also affect the outcome of this control.

Remark 2: If the start and goal locations change, the cost vector J^* has to be recomputed for the new start goal combination. The high convergence time of the MDP planner implies that it is not suitable in applications where the start-goal combinations change frequently. A similar argument applies if the forecast uncertainties are changed.

B. Minimum expected cost planner

The graph based minimum expected cost planned was used to compute a minimum expected cost path between the same start goal locations as the MDP planner. Since $\alpha = 2$, and $\sigma_{fx} = \sigma_{fy} = 0.09m/s$, a modified value of $K_h = K_h + K_d(\sigma_{fx}^2 + \sigma_{fy}^2 = 0.167$ was used with the STS method with $dT = 1000s$ to compute the path. Fig. 7 shows the computed path. The expected path cost was $7120J$, and the time required to compute this path was $3160s$. To verify the expected path cost, the obtained path was executed 100,000 times in simulations using the vehicle model given in (2), in a flow field with the same uncertainties as the ones used for the path computation, and the actual paths costs were recorded. Note that in these cost computations, the actual value of $K_d = 0.0005$ was used. The average expected path cost was $7120J$ and the standard deviation of the path cost was $427.1J$. The predicted standard deviation using (27) was $426.7J$. Thus it can be seen that the expected path costs and cost variances

TABLE I: Cost comparison of the three candidate paths

Path	Average Path Cost (J)	
	in deterministic flow	in uncertain flow
minExpCost	4304	7120
MDP	4258	7125
minDetCost	4219	7142

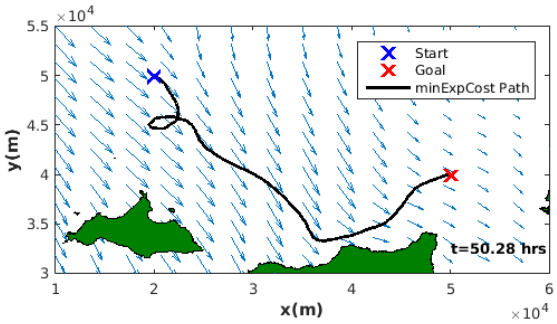

Fig. 7: Minimum expected cost path computed using the minimum expected cost planner. Expected path cost was $7120J$. The loop structure near $[20, 45]^T$ arises due to a circulation of the currents as it passes through that region.

predicted by (26) and (27) are accurate. Furthermore, in oder to verify that the path computed by the minimum expected cost planner actually has the minimum expected cost, three candidate paths were executed 100,000 times in simulations and the path cost statistics were recorded. The three candidate paths selected were, 1) **minExpCost** path: path obtained from the minimum expected cost planner, 2) **MDP** path: average path obtained from the MDP planner and 3) **minDetCost** path: path obtained in a deterministic flow (by setting $\sigma_{fx} = \sigma_{fx} = 0$). The path cost statistics for the three candidate paths are summarized in Table I. It can be seen that when the flow is fully known, the **minDetCost** path gives the minimum cost, and when the flow velocity forecasts are uncertain, the **minExpCost** path has the least expected cost.

VI. Conclusions

In this paper the problem of path planning under forecast uncertainty was addressed. Two methods to compute minimum expected cost policies and paths over an uncertain flow model were presented. A transition probability model was developed to compute the probability of transition from one state to another under a given action. Furthermore, a method to compute the expected cost of a path when it is executed in an uncertain flow field was also presented. The first planning method, the MPD planner, uses a Markov decision process to compute an optimal cost policy, while the second method, the minimum expected cost planner, uses the expected path segment cost in a graph search method to compute the minimum expected cost path. Both methods were used to compute minimum cost policies/paths in an ocean environment. The MDP planner outputs an optimal cost policy which can be used by the AMV to compute a control depending on its current state. It was seen that the

MDP planner is more suitable for applications in which the start/goal locations and the uncertainty levels are constant. However, since this method outputs a policy instead of a path, the actual execution cost might turn out to be lower than the cost of a path obtained by the minimum expected cost planner.

The graph based minimum cost planner on the other hand computes paths much faster, and as a result is more suited for applications where frequent path re-computations are necessary. Furthermore, it was seen that the path returned by this planner had the minimum average cost when executed in an uncertain flow field.

In this work it was assumed that the maximum AMV speed is always less than the maximum flow speed. Thus strong uncertain currents can advect the vehicle away from the computed minimum cost path and make the path inefficient and possibly infeasible. The effects of such large fluctuations on reachability and controllability in the minimum expected cost path planner needs to be further investigated.

The simulation results provided in this paper are based on assumed values for flow velocity uncertainties. It is worthwhile to investigate the performance of the presented methods in flows with known statistics. Thus experimentally validating the strategies within a flow field with known uncertainties is a direction for future work. Furthermore, similar to most other works in literature, we assume a Gaussian distribution for the uncertainty in the derivation of the proposed methods. The validity of such assumptions need to be investigated. Towards this end, we are currently looking at experimentally generating flow fields patterned on actual ocean flows, and analyzing the data to characterize uncertainty models.

REFERENCES

[1] J. Yuh, G. Marani, and D. R. Blidberg, "Applications of marine robotic vehicles," *Intelligent Service Robotics*, vol. 4, no. 4, p. 221, Jul 2011.

[2] B. Garau, A. Alvarez, and G. Oliver, "Path planning of autonomous underwater vehicles in current fields with complex spatial variability: an a* approach," in *Proc. of the 2005 IEEE International Conference on Robotics and Automation (ICRA2005)*, April 2005, pp. 194–198.

[3] D. Kularatne, S. Bhattacharya, and M. A. Hsieh, "Time and energy optimal path planning in general flows," in *Proceedings of Robotics: Science and Systems*, AnnArbor, Michigan, June 2016.

[4] ——, "Optimal path planning in time-varying flows using adaptive discretization," *IEEE Robotics and Automation Letters*, vol. 3, no. 1, pp. 458–465, Jan 2018.

[5] D. Kruger, R. Stolkin, A. Blum, and J. Briganti, "Optimal auv path planning for extended missions in complex, fast-flowing estuarine environments," in *Robotics and Automation, 2007 IEEE International Conference on*, April 2007, pp. 4265–4270.

[6] J. Witt and M. Dunbabin, "Go with the flow: Optimal auv path planning in coastal environments," in *Australasian Conference on Robotics and Automation (ACRA)*, 2008.

[7] T. Lolla, P. F. J. Lermusiaux, M. P. Ueckermann, and P. J. Haley, "Time-optimal path planning in dynamic flows using level set equations: theory and schemes," *Ocean Dynamics*, vol. 64, no. 10, pp. 1373–1397, 2014.

[8] D. N. Subramani and P. F. Lermusiaux, "Energy-optimal path planning by stochastic dynamically orthogonal level-set optimization," *Ocean Modelling*, vol. 100, pp. 57 – 77, 2016.

[9] Regional ocean model system (roms) model output. [Online]. Available: http://www.sccoos.org/data/roms-3km/

[10] T. Sondergaard and P. F. J. Lermusiaux, "Data assimilation with gaussian mixture models using the dynamically orthogonal field equations. part i: Theory and scheme," *Monthly Weather Review*, vol. 141, no. 6, pp. 1737–1760, 2013.

[11] V. Huynh, M. Dunbabin, and R. Smith, "Predictive motion planning for auvs subject to strong time-varying currents and forecasting uncertainties," in *Robotics and Automation (ICRA), 2015 IEEE International Conference on*, 2015, pp. 1144–1151.

[12] W. H. Al-Sabban, L. F. Gonzalez, and R. N. Smith, "Wind-energy based path planning for unmanned aerial vehicles using markov decision processes," in *Robotics and Automation (ICRA), 2013 IEEE International Conference on*, May 2013, pp. 784–789.

[13] M. T. Wolf, L. Blackmore, Y. Kuwata, N. Fathpour, A. Elfes, and C. Newman, "Probabilistic motion planning of balloons in strong, uncertain wind fields," in *2010 IEEE International Conference on Robotics and Automation*, May 2010, pp. 1123–1129.

[14] A. A. Pereira, J. Binney, G. A. Hollinger, and G. S. Sukhatme, "Risk-aware path planning for autonomous underwater vehicles using predictive ocean models," *Journal of Field Robotics*, vol. 30, no. 5, pp. 741–762, 2013. [Online]. Available: http://dx.doi.org/10.1002/rob.21472

[15] B. Bonet, "On the speed of convergence of value iteration on stochastic shortest-path problems," *Mathematics of Operations Research*, vol. 32, no. 2, pp. 365–373, 2007. [Online]. Available: https://doi.org/10.1287/moor.1060.0238

[16] D. Kularatne, S. Bhattacharya, and M. A. Hsieh, "Computing energy optimal paths in time-varying flows," Drexel University, Philadelphia, USA, Tech. Rep., 2016, doi:10.17918/D8B66V.